Astronomy Letters, Vol. 28, No. 6, 2002, pp. 353–365. Translated from Pis'ma v Astronomicheskiĭ Zhurnal, Vol. 28, No. 6, 2002, pp. 403–416.

A Catalog of Cosmic Gamma-Ray Bursts Detected by the PHEBUS Instrument on the Granat Observatory: October 1994–December 1996

A. Yu. Tkachenko[1*], O. V. Terekhov[1], R. A. Sunyaev[1], A. V. Kuznetsov[1], C. Barat[2], J.-P. Dezalay[2], and G. Vedrenne[2]

[1]*Space Research Institute, Russian Academy of Sciences, Profsoyuznaya ul. 84/32, Moscow, 117810 Russia*

[2]*Centre d'Etude Spatiale des Rayonnements, 9 avenue du Colonel Roche, BP 4346, 31028 Toulouse Cedex 4, France*

Received January 17, 2002

Abstract—We present the final part of the catalog of cosmic gamma-ray bursts (GRBs) observed in the PHEBUS experiment on the Granat orbiting astrophysical observatory. The first three parts of the catalog were published by Terekhov *et al.* (1994, 1995a) and Tkachenko *et al.* (1998). The fourth part contains information on 32 events recorded from October 1994 until December 1996. We give burst light curves in the energy range 100 keV to 1.6 MeV, integrated energy spectra, and information on the fluence and energy flux at the luminosity peak for energies above 100 keV. Over the entire period of its operation, the PHEBUS instrument detected 206 cosmic GRBs. The mean $\langle V/V_{\rm max}\rangle$ was 0.336 ± 0.007. The mean hardness corresponding to the ratio of count numbers in the energy ranges 400–1000 and 100–400 keV is 0.428 ± 0.018 for events with a duration shorter than 2 s and 0.231 ± 0.004 for events with a duration longer than 2 s. © *2002 MAIK "Nauka/Interperiodica"*.

Key words: *gamma-ray bursts, catalog*

INTRODUCTION

The PHEBUS instrument was devised at the Centre d'Etude Spatiale des Rayonnements in Toulouse (France) and installed onboard the Granat orbiting astrophysical observatory, which was launched into a high-apogee orbit on December 1, 1989. The instrument was designed to study cosmic gamma-ray bursts (GRBs) and high-energy solar flares in the energy range 100 keV to 100 MeV. It consisted of six bismuth germanate (BGO) detectors surrounded by a plastic anticoincidence shield. The detectors were located on different sides of the Granat observatory. PHEBUS had successfully operated in orbit and recorded burst events until late 1996. A detailed description of the instrument and the modes of its operation can be found in Barat *et al.* (1988).

The previous parts of the catalog contain the results of the PHEBUS observations of cosmic GRBs from December 1989 until September 1994 (Terekhov *et al.* 1994, 1995a; Tkachenko *et al.* 1998). This part presents the results of the GRB observations from October 1994 until December 1996. The data reduction technique and presentation of the results are the same as those in the previous parts of the catalog. In general, the catalog structure was also preserved. Explanations on modifications are given in the text of the catalog.

THE STATISTICS OF RECORDED EVENTS

Since October 1994, the Granat observatory spent most of the time in scanning mode and PHEBUS was not switched off during its passage through the Earth's radiation belts. The number of burst events whose information could be written to the PHEBUS onboard memory was limited; therefore, such a mode of operation resulted in a reduction in the number of detected GRBs. Magnetospheric events accounted for most of the PHEBUS burst cell triggerings.

The total observing time from October 1994 until December 1996 was 164 days. Over this period, 428 PHEBUS burst cell triggerings were recorded. Only 32 of them were related to cosmic GRBs and two were related to X-ray solar flares. The light curves of some high-energy solar flares are similar to those of cosmic GRBs and their energy spectra may extend beyond a few hundred keV and, in some cases, up to several tens of MeV (Terekhov *et al.* 1995b). We selected GRBs from all of the events recorded during the experiment by using the confirmations of the events by other spaceborne observatories. Over the entire period of its operation (December 1989–December 1996), PHEBUS obtained information on 206 cosmic GRBs.

*E-mail: ayut@hea.iki.rssi.ru

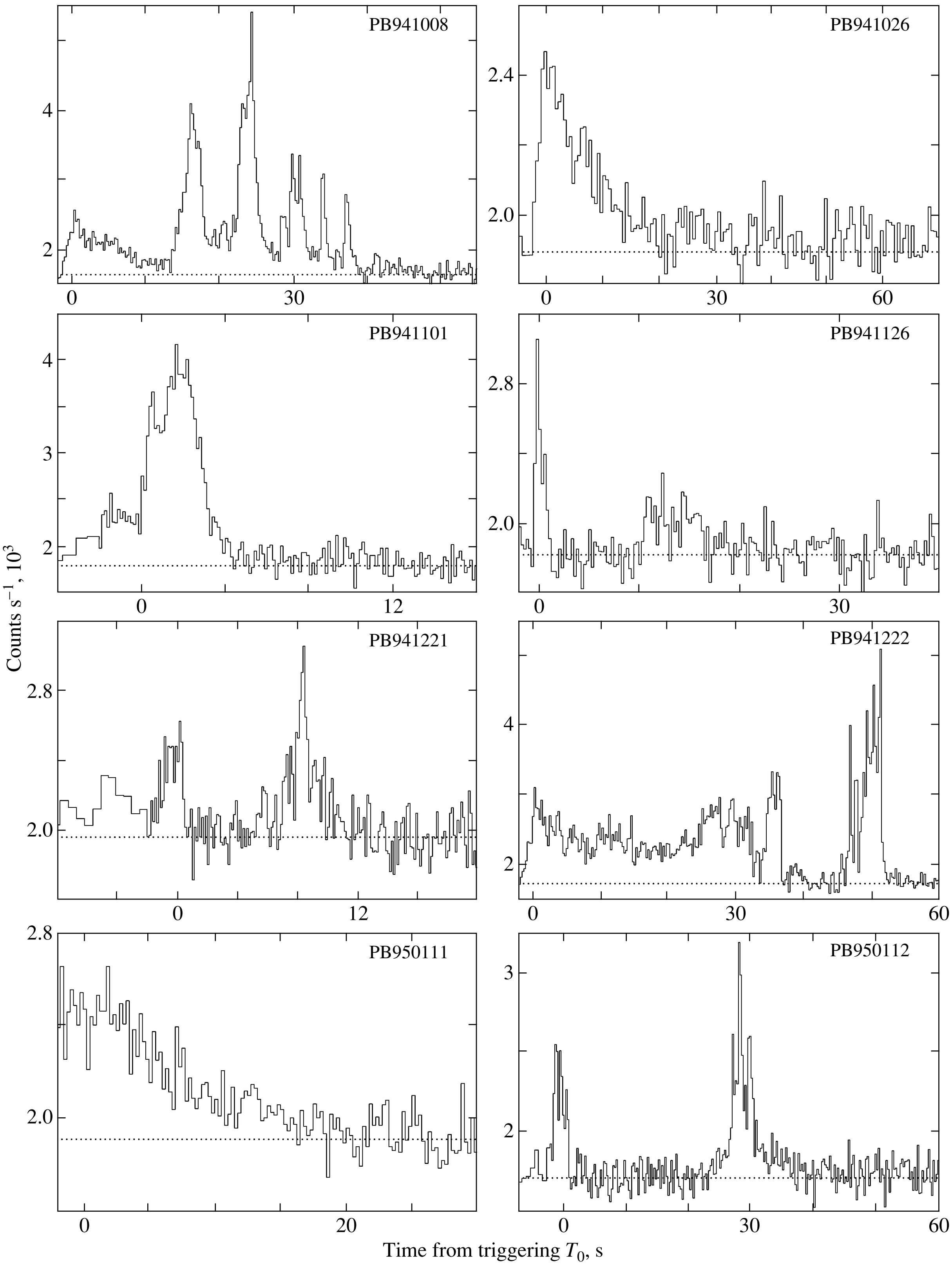

Fig. 1. Light curves of the cosmic GRBs detected by the PHEBUS instrument on the Granat observatory from October 1994 until December 1996 in the energy range 100 keV to 1.6 MeV. The dotted line indicates the PHEBUS detector background levels in a period immediately preceding the burst.

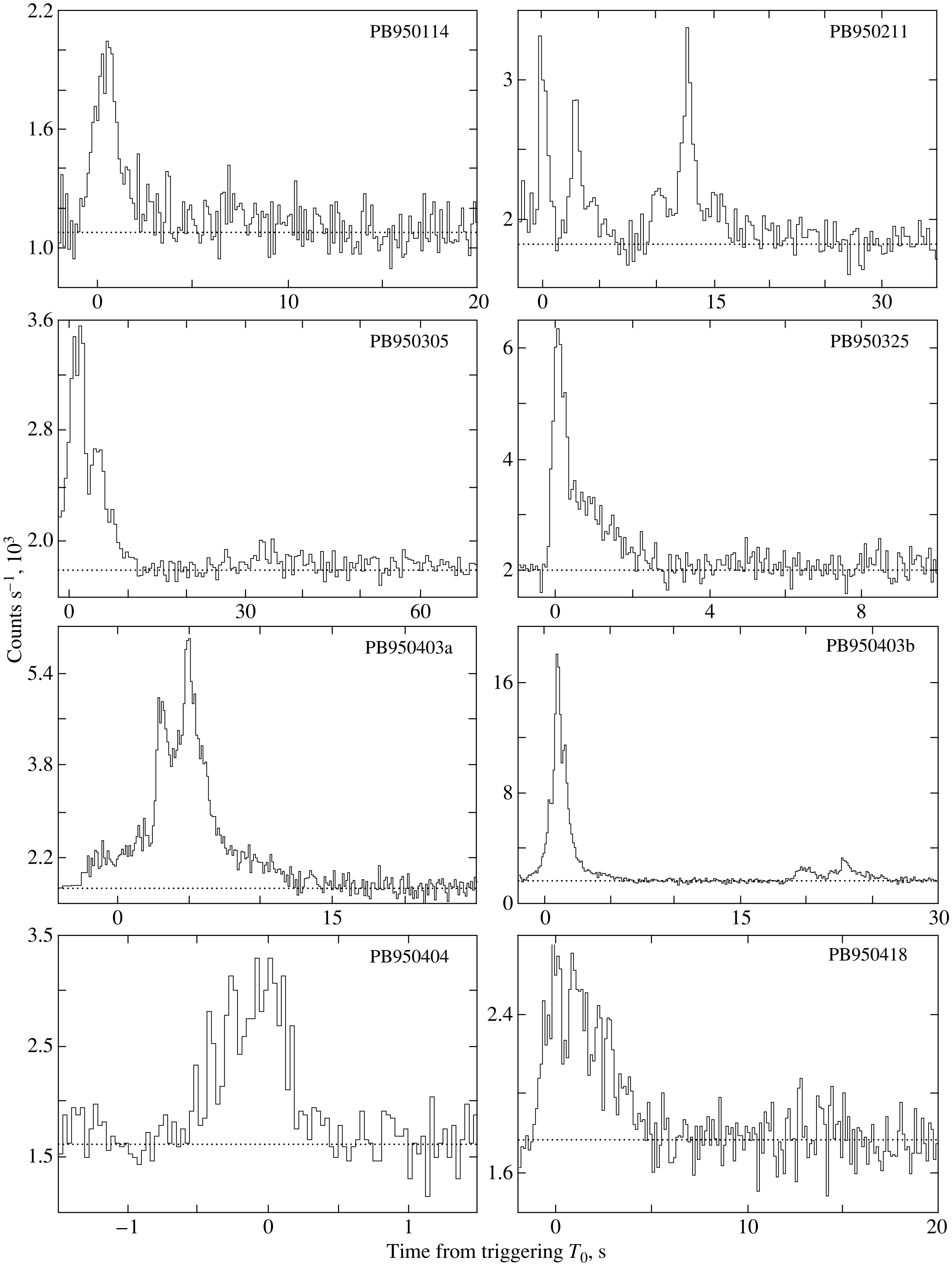

PB950114
PB950211
PB950305
PB950325
PB950403a
PB950403b
PB950404
PB950418
Counts s^{-1}, 10^3
Time from triggering T_0, s

Fig. 1. (Contd.)

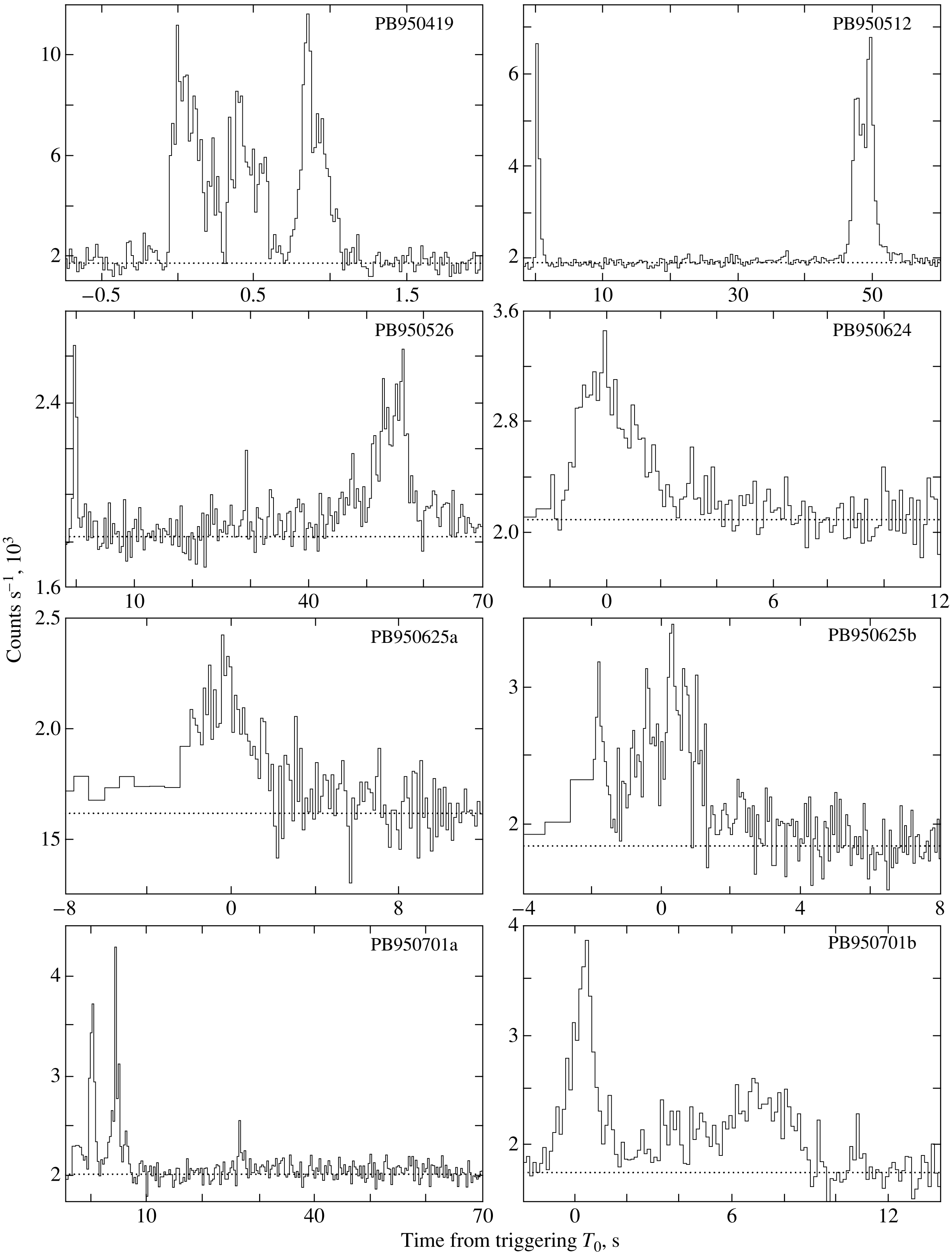
PB950419
PB950512
PB950526
PB950624
PB950625a
PB950625b
PB950701a
PB950701b
Counts s^{-1}, 10^{3}
Time from triggering T_0, s

Fig. 1. (Contd.)

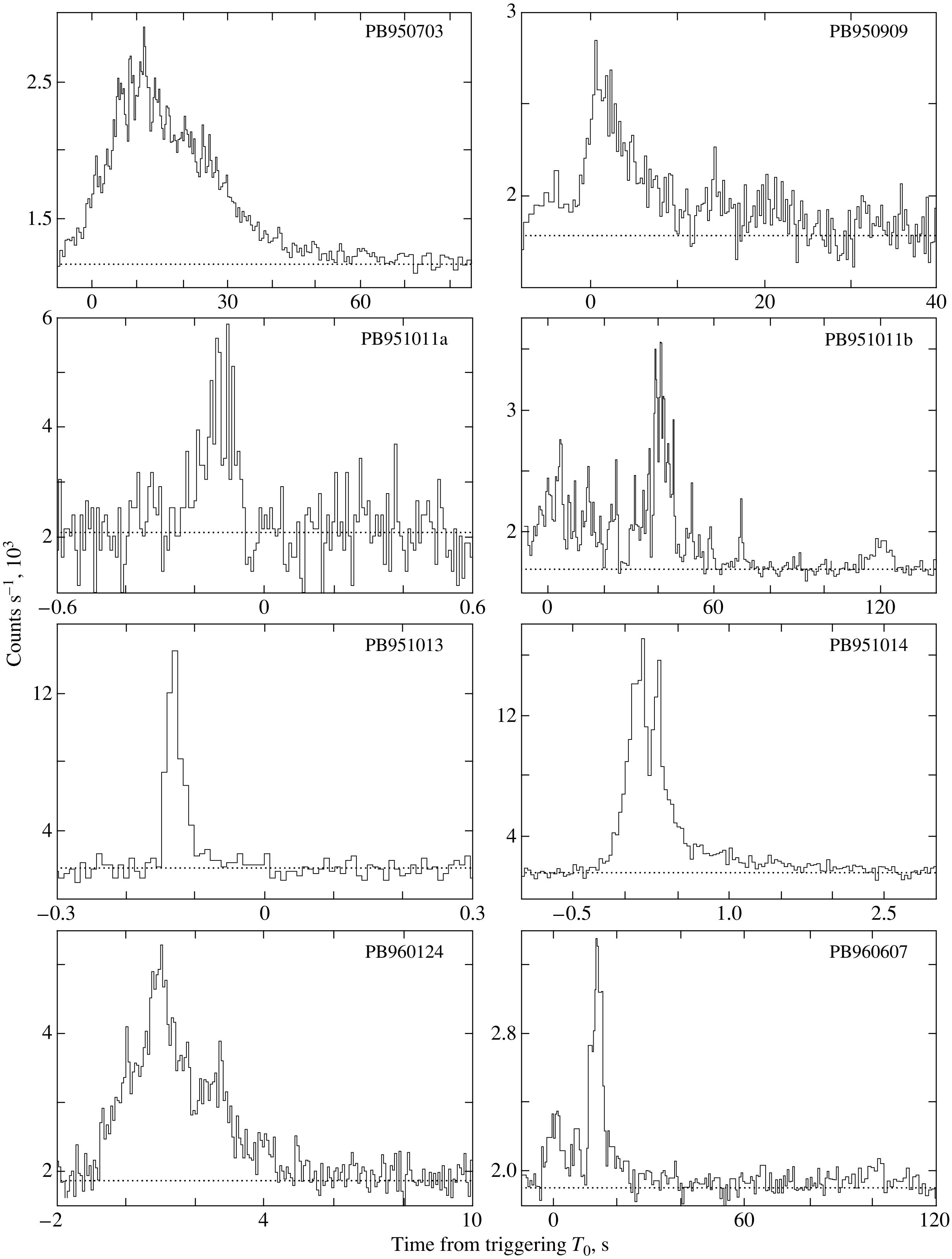
PB950703
PB950909
PB951011a
PB951011b
PB951013
PB951014
PB960124
PB960607
Counts s^{-1}, 10^3
Time from triggering T_0, s
2.5
1.5
0
30
60
3
2
0
20
40
6
4
2
−0.6
0
0.6
3
2
0
60
120
12
4
−0.3
0
0.3
12
4
−0.5
1.0
2.5
4
2
−2
4
10
2.8
2.0
0
60
120

Fig. 1. (Contd.)

Main characteristics of 32 GRBs detected by the PHEBUS instrument (October 1994–December 1996)

Burst name	Session number	Triggering time	Duration T_{90}, s	$C_{\max}/C_{\min}$	Fluence[a], 10^{-5} erg cm^{-2}	Peak flux[a], 10^{-5} erg cm^{-2} s^{-1}	Spectral hardness[b]	Anal. law	Para-meter	χ^2/DOF	Notes[c]
PB941008	805.01	$13^{h}34^{m}18^{s}.685$	36.19 ± 0.32	5.89 ± 0.29	16.07 ± 6.06	4.10 ± 1.80	0.26 ± 0.01	S	2.69	67.19/33	BU
PB941026	807.01	2 52 37 629	58.86 ± 1.10	1.22 ± 0.20	0.62 ± 0.24	0.31 ± 0.14	0.15 ± 0.04	S	1.32	7.17/9	B
PB941101	809.01	6 30 58 595	12.56 ± 1.26	4.70 ± 0.26	3.31 ± 1.28	1.33 ± 0.57	0.15 ± 0.01	P	−1.97	19.68/17	U
PB941126	812.01	0 20 46 130	23.13 ± 0.20	1.24 ± 0.22	1.56 ± 0.71	1.89 ± 0.90	0.60 ± 0.12	P	−1.36	3.00/8	BK
PB941221	819.01	22 14 36 608	11.40 ± 0.48	1.26 ± 0.20	0.74 ± 0.33	0.25 ± 0.10	0.15 ± 0.06	P	−1.52	12.35/8	K
PB941222	819.02	5 36 53 894	49.99 ± 0.22	4.92 ± 0.27	42.22 ± 17.83	3.16 ± 1.25	0.44 ± 0.01	S	6.53	115.77/40	K
PB950111	821.04	12 18 47 790	18.82 ± 1.46	1.29 ± 0.20	1.47 ± 0.56	0.29 ± 0.13	0.27 ± 0.04	S	1.36	6.54/14	BK
PB950112	821.05	7 45 41 212	51.47 ± 0.83	1.97 ± 0.21	2.16 ± 0.86	1.30 ± 0.60	0.15 ± 0.02	P	−1.98	8.11/9	K
PB950114	822.01	13 10 32 276	8.67 ± 0.67	4.04 ± 0.25	0.93 ± 0.35	0.77 ± 0.30	0.09 ± 0.02	P	−2.56	7.24/10	KUT
PB950211	829.01	20 08 20 819	23.45 ± 1.06	2.40 ± 0.22	1.71 ± 0.69	0.71 ± 0.35	0.15 ± 0.02	P	−1.97	18.94/11	BKU
PB950305	835.01	15 05 17 909	58.97 ± 1.00	3.15 ± 0.23	3.08 ± 1.20	0.56 ± 0.22	0.29 ± 0.03	S	2.29	12.91/18	BK
PB950325	837.01	7 10 44 283	6.47 ± 0.84	4.14 ± 0.24	2.07 ± 0.82	2.35 ± 0.95	0.30 ± 0.03	S	3.49	30.99/19	BKU
PB950403a	842.01	13 19 50 238	11.26 ± 0.41	6.66 ± 0.30	9.85 ± 3.76	1.57 ± 0.61	0.19 ± 0.01	P	−2.14	40.42/26	BKUY
PB950403b	842.02	23 33 50 352	23.42 ± 0.19	20.01 ± 0.61	15.72 ± 5.99	12.23 ± 4.73	0.21 ± 0.01	S	2.04	55.80/33	BKUD
PB950404	842.03	3 23 32 240	1.65 ± 0.65	1.68 ± 0.21	0.27 ± 0.13	0.54 ± 0.26	0.24 ± 0.07	P	−1.90	8.32/7	
PB950418	844.01	23 16 35 985	13.67 ± 2.70	1.94 ± 0.21	1.21 ± 0.46	0.42 ± 0.18	0.22 ± 0.03	S	3.05	12.55/14	BK
PB950419	844.02	2 23 46 686	1.04 ± 0.03	9.62 ± 0.38	3.10 ± 1.19	6.13 ± 2.38	0.31 ± 0.02	S	3.59	29.39/28	KU
PB950512	848.01	0 16 48 150	51.25 ± 0.33	9.77 ± 0.33	17.01 ± 7.17	2.96 ± 1.14	0.19 ± 0.01	S	2.78	31.22/21	KUS
PB950526	849.01	4 36 57 281	62.11 ± 0.46	1.45 ± 0.20	1.19 ± 0.51	0.57 ± 0.29	0.32 ± 0.05	P	−1.31	3.28/8	K
PB950624	855.01	23 22 05 401	7.56 ± 0.62	1.74 ± 0.20	1.09 ± 0.47	0.36 ± 0.16	0.20 ± 0.04	P	−1.88	8.28/9	BK
PB950625a	855.02	4 03 42 561	8.31 ± 1.26	1.17 ± 0.20	0.49 ± 0.19	0.23 ± 0.10	0.09 ± 0.04	P	−2.22	1.85/8	BK
PB950625b	855.03	5 19 35 248	5.49 ± 0.61	1.66 ± 0.20	0.70 ± 0.27	0.38 ± 0.15	0.09 ± 0.03	P	−2.48	13.96/9	K
PB950701a	856.03	3 32 41 722	57.26 ± 1.65	2.56 ± 0.22	1.84 ± 0.73	0.73 ± 0.28	0.24 ± 0.03	S	3.64	11.80/16	BKUY
PB950701b	856.04	6 35 37 770	8.83 ± 0.19	2.58 ± 0.22	0.98 ± 0.38	0.43 ± 0.17	0.17 ± 0.03	S	1.98	10.69/11	BKU
PB950703	856.05	5 33 42 000	45.28 ± 1.74	4.15 ± 0.26	21.21 ± 8.01	0.97 ± 0.38	0.22 ± 0.01	B	506.08	58.55/28	KD
PB950909	867.01	23 44 38 894	32.14 ± 5.57	1.79 ± 0.20	2.36 ± 0.95	0.19 ± 0.08	0.32 ± 0.04	S	2.33	14.19/16	BK
PB951011a	876.01	0 44 37 284	0.25 ± 0.06	1.02 ± 0.21	0.12 ± 0.06	0.25 ± 0.11	0.39 ± 0.17	P	−1.37	2.97/4	
PB951011b	876.03	21 34 55 420	119.41 ± 1.55	3.41 ± 0.23	19.48 ± 7.55	1.38 ± 0.58	0.31 ± 0.01	S	2.09	31.95/28	BKD
PB951013	876.04	15 51 37 022	0.09 ± 0.04	1.14 ± 0.21	0.28 ± 0.13	0.66 ± 0.32	0.37 ± 0.12	P	−1.52	0.93/3	K
PB951014	876.05	3 38 26 193	1.58 ± 0.11	12.63 ± 0.62	17.43 ± 9.00	10.06 ± 3.89	0.30 ± 0.02	S	3.88	51.81/32	KTU
PB960124	888.01	0 56 28 045	7.03 ± 0.56	4.05 ± 0.25	4.14 ± 1.58	2.39 ± 1.04	0.20 ± 0.02	P	−1.84	44.60/22	BKUT
PB960607	909.01	21 41 49 791	103.34 ± 1.60	2.55 ± 0.22	3.25 ± 1.32	0.41 ± 0.16	0.21 ± 0.03	P	−2.09	3.76/10	BKU

[a] The fluence and peak flux at energy above 100 keV.

[b] The hardness of the integrated energy spectra defined as the ratio of count numbers in the ranges 400–1000 and 100–400 keV.

[c] The burst was observed by other instruments: (B) BATSE, (K) KONUS/WIND, (T) TGRS/WIND, (U) ULYSSES, (Y) YOHKOH, (D) DMS, (S) SROSS-C.

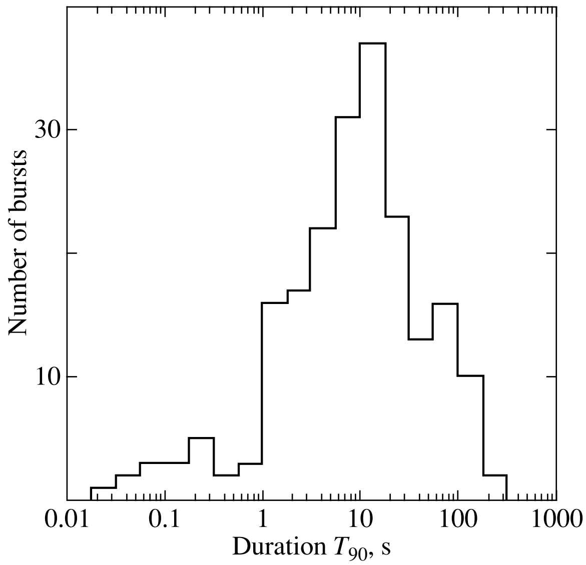

Fig. 2. The T_{90} distribution of 206 GRBs detected over the entire period of PHEBUS operation.

The table lists temporal and spectral characteristics of 32 GRBs detected over the period under consideration. For each event, it gives the burst detection date, the number of the Granat session in which this event was recorded, and the Universal Time T_0 of the PHEBUS burst cell triggering.

The Notes column gives information on the recording of these events by the burst instruments of other satellites: BATSE, KONUS/WIND, TGRS/WIND, ULYSSES, YOHKOH, DMS (Defense Meteorite Satellite Program), and SROSS-C. When compiling the list of confirmations, we used data from the Web page http://ssl.berkeley.edu/ipn3/masterli.txt.

BURST TEMPORAL CHARACTERISTICS

Figure 1 shows the GRB light curves in the energy range 100 keV to 1.6 MeV. The time was measured from the PHEBUS burst cell triggering T_0. The count rate was determined as a sum of the count rates of three detectors in which the count rate was at a maximum. We chose the time interval and time resolution for each event individually, because the burst temporal structure and duration varied widely. Note that because of the Granat high-apogee orbit, the detector background was highly constant and its variations on time scales of the order of the characteristic burst duration (1–100 s) were negligible.

The table lists the burst durations defined by T_{90}. This parameter is the interval between the times when 5 and 95% of the total burst energy was released; it is commonly used to measure the burst durations. Figure 2 presents the T_{90} distribution of 206 GRBs detected over the entire period of PHEBUS operation. Similar to other experiments (Kouveliotou *et al.* 1993), there are two peaks in this distribution. This bimodal pattern in the duration distribution of GRBs may suggest that the sources of short and long events are different in nature.

$\langle V/V_{\max}\rangle$. One of the uniformity criteria for the spatial distribution of GRBs is the $\langle V/V_{\max}\rangle$ ratio, where V is the volume of the minimum sphere containing a burst and $V_{\max}$ is the maximum volume of space accessible to burst detection at a given time (Schmidt *et al.* 1988; Higdon and Schmidt 1990). The value of $V_{\max}$ is determined by the instrument sensitivity. For a spatially uniform distribution of the sources, $\langle V/V_{\max}\rangle$ must be 1/2. If $C_{\max}$ is the maximum count rate recorded during a burst and $C_{\min}$ is the threshold count rate at which the event will be detected, then $V/V_{\max} = (C_{\min}/C_{\max})^{3/2}$.

For the PHEBUS bursts, $C_{\max}/C_{\min}$ was calculated for each of the six detectors. The burst signal could be generated on two time scales (0.25 and 1 s). We computed $C_{\max}/C_{\min}$ on these two scales and then determined on which of them a maximum was reached in a given detector. To determine the mean ratio $\langle V/V_{\max}\rangle$, we used not the maximum value but the second largest value of $C_{\max}/C_{\min}$ among the six detectors on the chosen time scale, because the triggering of the PHEBUS burst detection circuit required that the threshold be exceeded in at least two detectors. The values of $C_{\max}/C_{\min}$ obtained for each burst are given in the table.

For the events recorded by PHEBUS from October 1994 until December 1996, we obtained $\langle V/V_{\max}\rangle = 0.336 \pm 0.018$. The mean value of $V/V_{\max}$ for all of the 206 GRBs detected over the entire period of PHEBUS operation is 0.336 ± 0.007. This value differs from 1/2 expected for a uniform distribution of GRB sources in Euclidean space by more than 23 standard deviations. The derived value is in agreement with the data of other experiments (Hurley 1992; Ogasaka *et al.* 1991; Atteia *et al.* 1991; Mitrofanov *et al.* 1992; Dezalay *et al.* 1994; Meegan *et al.* 1996; Paciesas *et al.* 1999).

GRB SPECTRAL CHARACTERISTICS

For each GRB, the table gives the fluence and peak flux at energy above 100 keV. The errors in the fluxes are not only statistical: we also took into account the uncertainty in the PHEBUS effective area attributable to the unknown position of the GRB source in the sky. Also given in the table is the hardness of the integrated energy spectra, defined as the ratio of count numbers in the energy ranges 400–1000 and 100–400 keV.

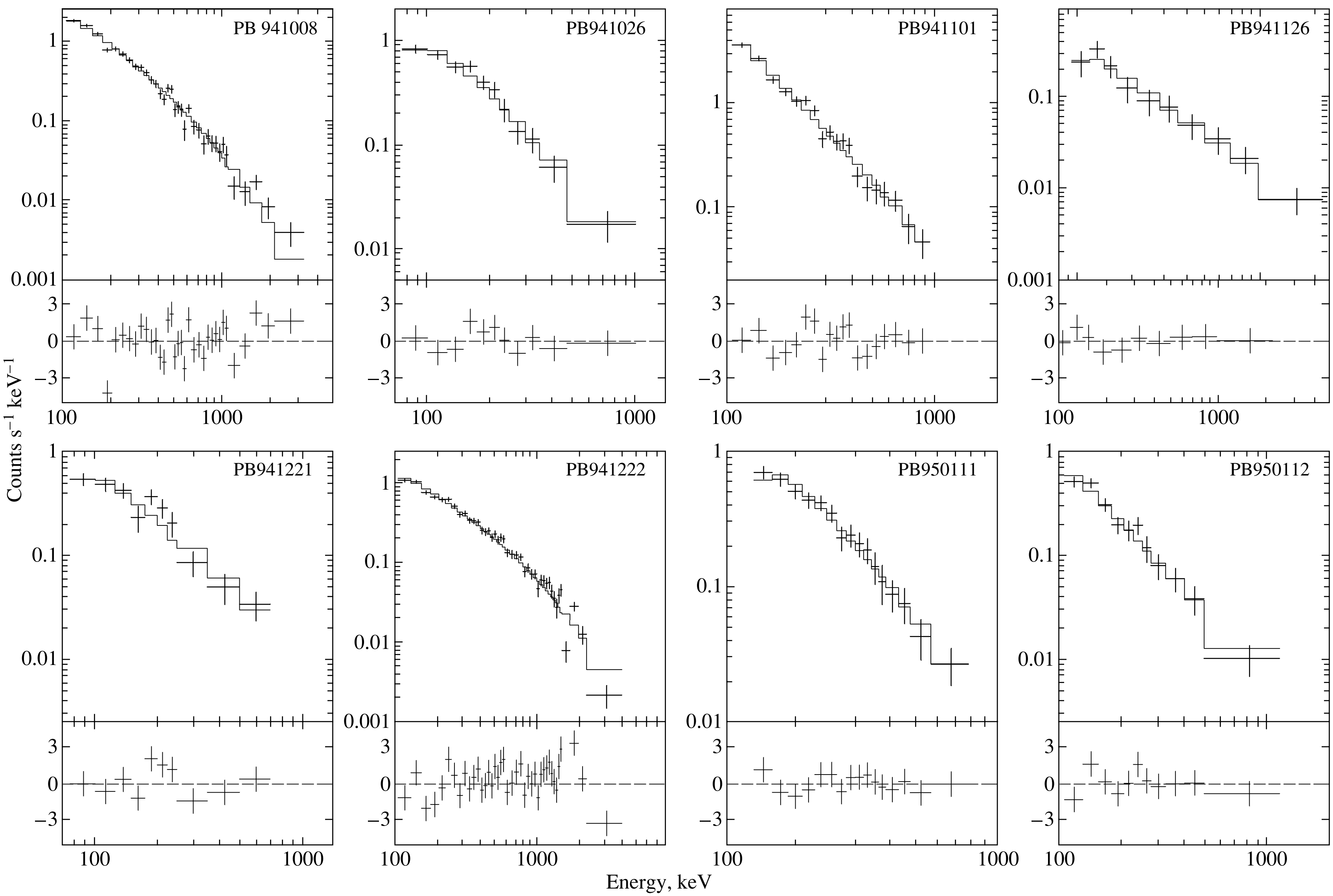

Fig. 3. Time-integrated energy spectra for all 32 GRBs. The broken line represents the best fit to the data (see the text). The lower panel of each figure shows deviations of the experimental data from the analytic curve, in units of standard deviations (σ).

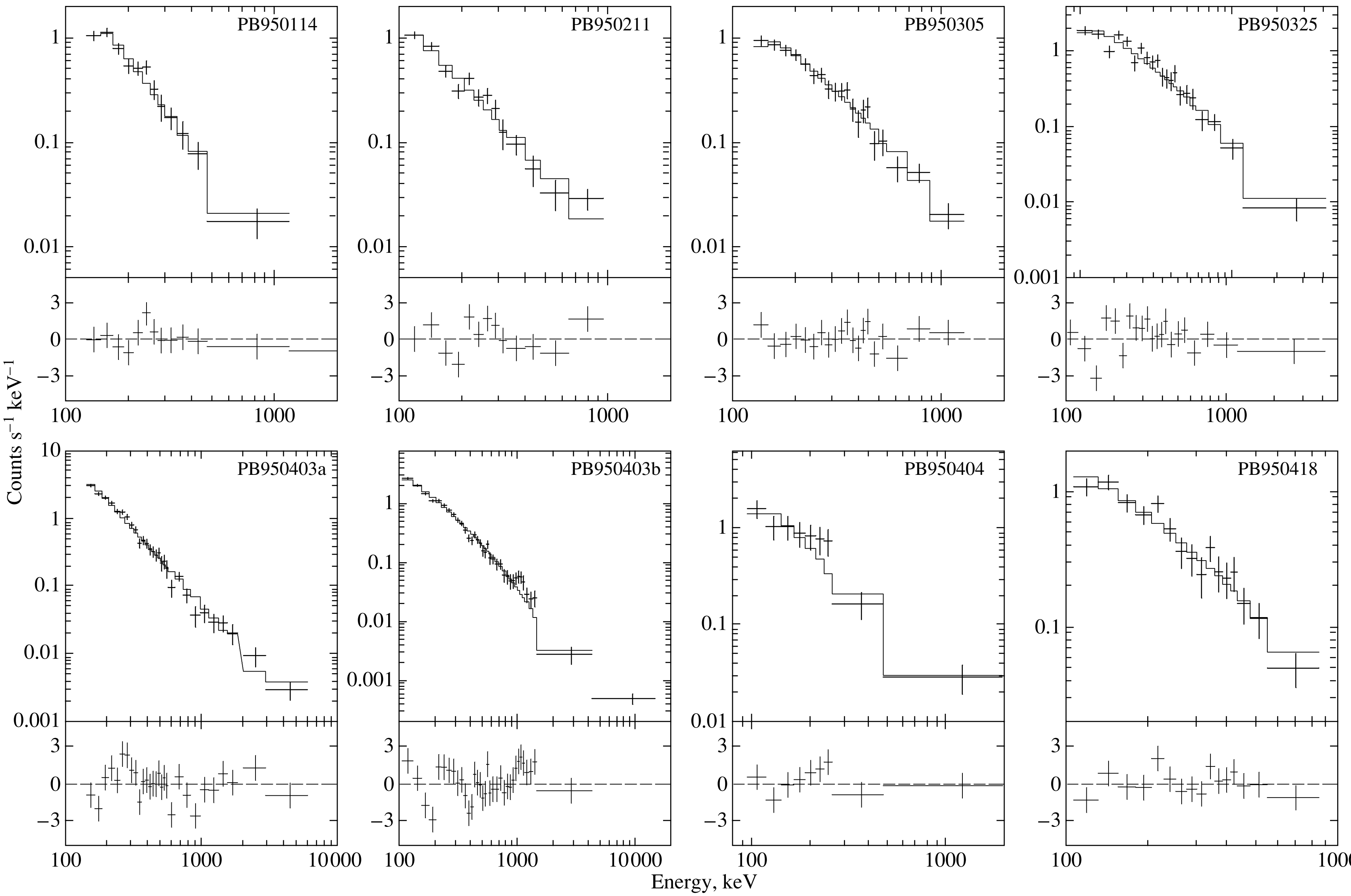
PB950114
PB950211
PB950305
PB950325
PB950403a
PB950403b
PB950404
PB950418
Counts s^{-1} keV^{-1}
Energy, keV

Fig. 3. (Contd.)

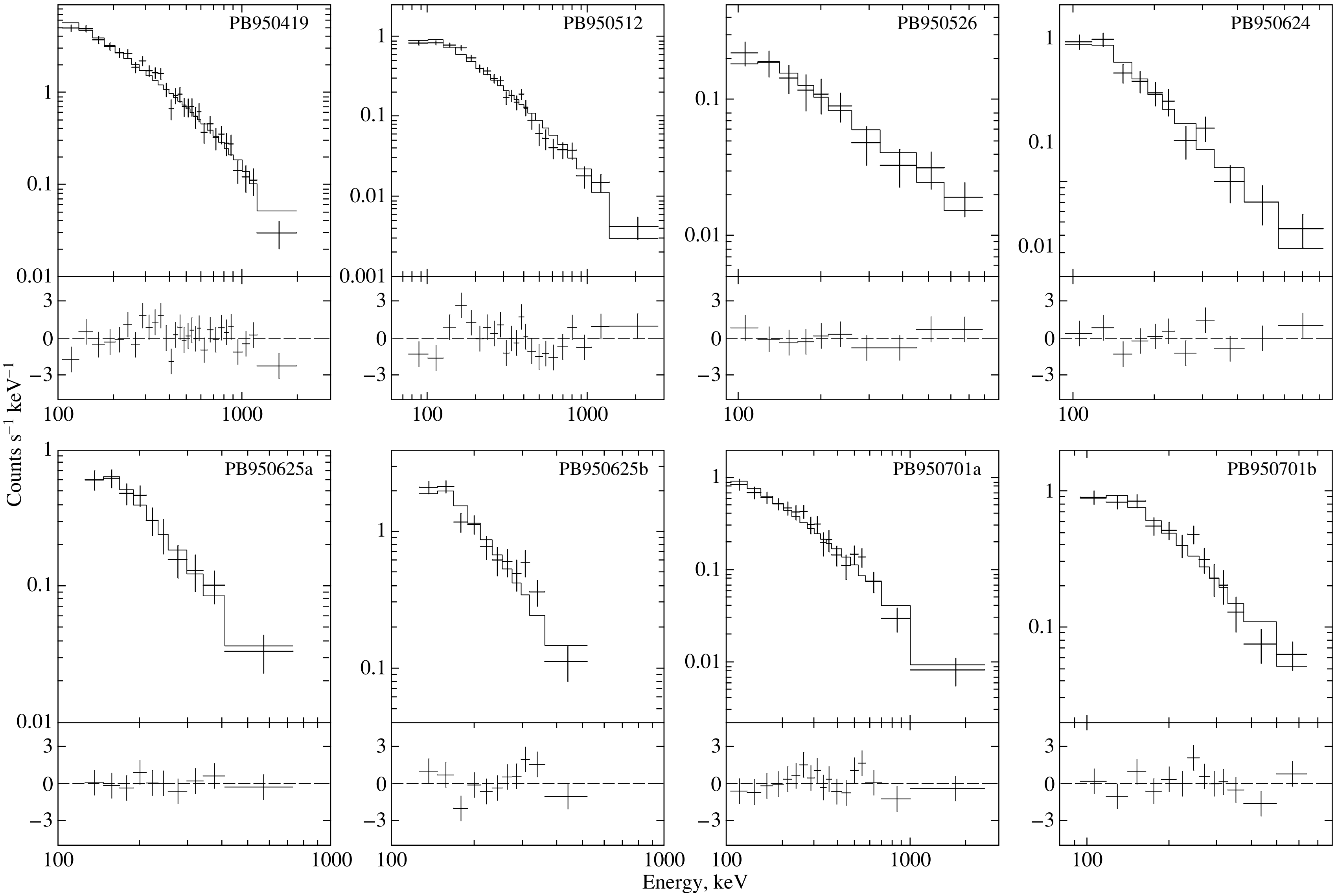
PB950419
PB950512
PB950526
PB950624
PB950625a
PB950625b
PB950701a
PB950701b
Counts s⁻¹ keV⁻¹
Energy, keV

Fig. 3. (Contd.)

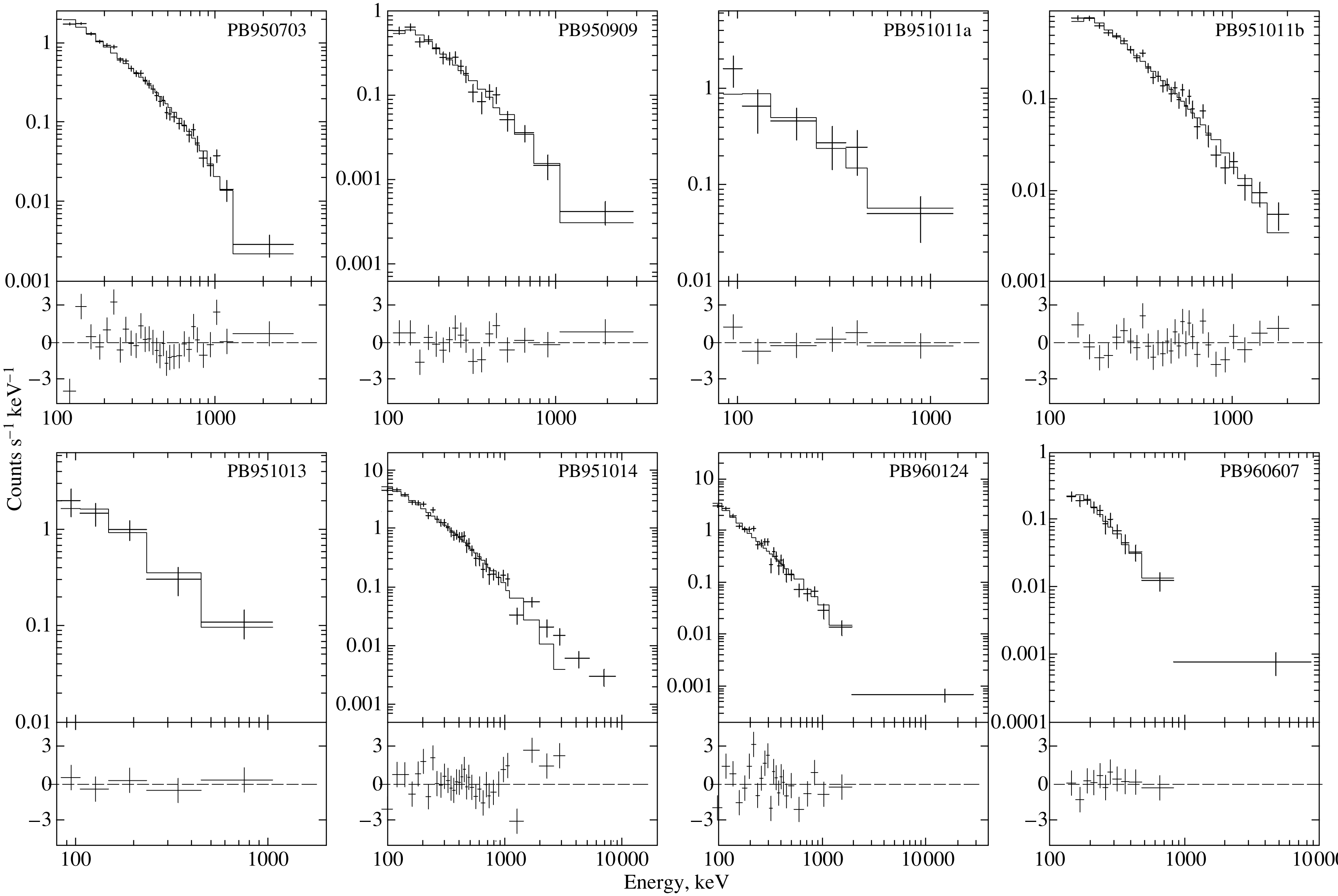
PB950703
PB950909
PB951011a
PB951011b
PB951013
PB951014
PB960124
PB960607
Counts s^{-1} keV^{-1}
Energy, keV

Fig. 3. (Contd.)

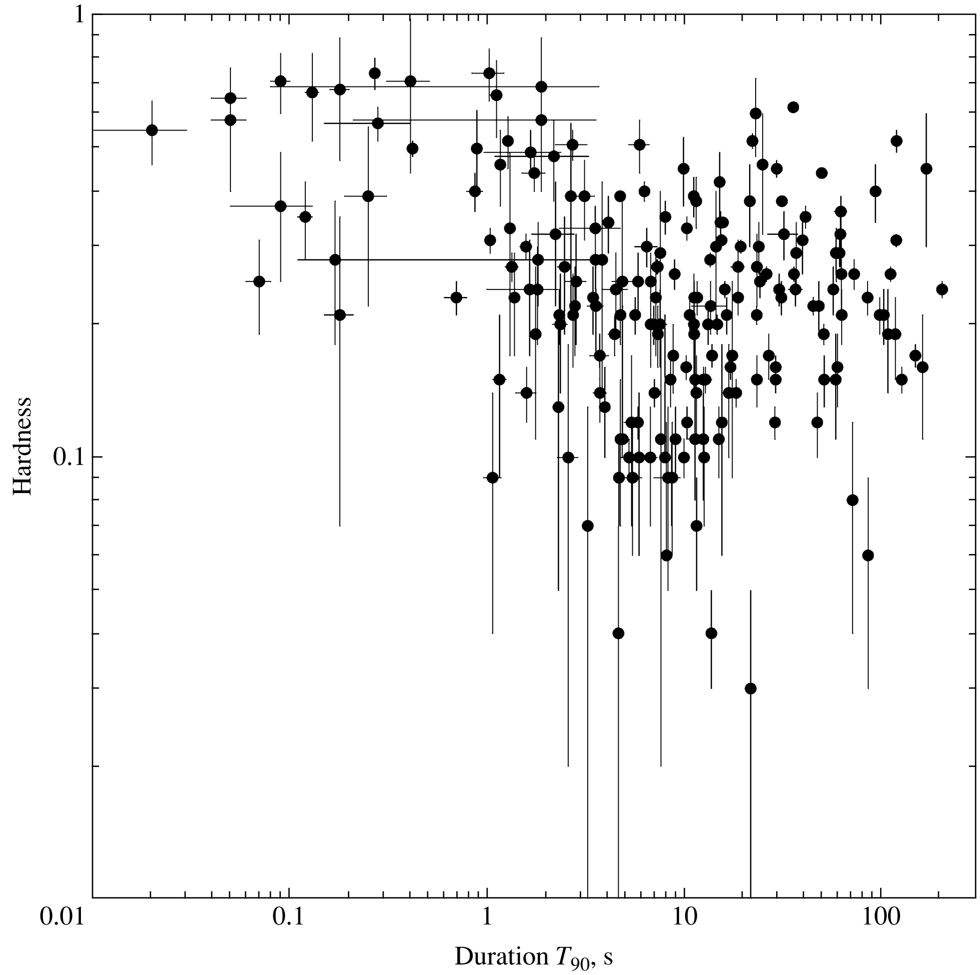

Fig. 4. Burst hardness *versus* burst duration T_{90}. The mean hardness for bursts with durations shorter and longer than 2 s is 0.428 ± 0.018 and 0.231 ± 0.008, respectively.

Figure 3 shows time-integrated energy spectra for the 32 GRBs of this catalog. The integration time is T_{90}. For a convenient comparison of the slopes in the spectra, we chose the scales on the horizontal and vertical axes in all figures in such a way that the diagonal running from the upper left corner to the lower right corner corresponded to a power law with an index of -2. The broken line is the best fit to the data by one of the following functions: the power law $I(E) = AE^p$, where E is the photon energy, p is the exponent; the bremsstrahlung law $I(E) = A\exp(-E/kT)/E$, where T is the characteristic temperature, k is the Boltzmann constant; and the synchrotron radiation law $I(E) = A\exp\{-(E/E_c)^{1/3}\}$, where $E_c = 4.5^{-1}\omega_{\rm H}\sin\Theta(kT/mc^2)^2$, $\omega_{\rm H}$ is the electron gyrofrequency, and Θ is the angle between the direction of photon motion and the magnetic field (Petrosian 1981).

We chose these laws, because they are most commonly used to fit the burst energy spectra in the energy range under study (Mazets and Golenetskiĭ 1987; Petrosian 1981; Schaefer *et al.* 1994).

We determined the best fit and sought for its parameters by using the χ^2 test. The table lists the best fits to the spectral data: the power law (P), the bremsstrahlung law (B), and the synchrotron radiation law (S). The next columns give their parameters: the dimensionless exponent p; the characteristic temperature kT (in keV) or the parameter E_c (in keV), respectively; and the χ^2/DOF ratio that characterizes the spectrum fitting reliability, where DOF is the number of degrees of freedom.

The hardness is one of the parameters used to investigate GRB spectra and to classify events. This parameter carries information on the fraction of the high-energy photons in the burst energy spectrum, although it gives no idea of the spectral shape.

It has already been noted previously (Dezalay *et al.* 1992; Terekhov *et al.* 1994, 1995a; Kouveliotou *et al.* 1993) that the mean hardness of short bursts is higher than that of long bursts. In Fig. 4, burst hardness is plotted against burst duration. The mean hardness for the cosmic GRBs detected by PHEBUS over the entire period of its operation is 0.428 ± 0.018 for events shorter than 2 s and 0.231 ± 0.004 for events longer than 2 s. The result obtained, as well as the bimodal pattern of the GRB distribution in duration, may suggest that the sources of short and long bursts are different in nature.

ACKNOWLEDGMENTS

This study was supported by the Russian Foundation for Basic Research (project no. 00-02-17251), the Program "Astronomy: Nonstationary Astrophysical Objects" of the Russian Academy of Sciences, and the sixth Examination Competition in 1999 and the Science Support Foundation Grant for Talented Young Researchers. We wish to thank the staff of the Lavochkin Research and Production Association, *Radiopribor* Research and Production Association, the Deep Space Communication Center in Eupatoria, B.S. Novikov, V.I. Evgenov, A.N. Bogomolov, N.G. Khavensonthe from the Space Research Institute (Russian Academy of Sciences) who operated the observatory, and the team of A.V. D'yachkov who processed the telemetry information. We are grateful to E.P. Mazets, R.A. Aptekar', and S.V. Golenetskiĭ from the Ioffe Physicotechnical Institute, Russian Academy of Sciences (St. Petersburg) who provided data on the KONUS/WIND confirmation of several GRBs under discussion.

REFERENCES

1. J.-L. Atteia, C. Barat, E. Jourdain, *et al.*, Nature **351**, 296 (1991).
2. C. Barat, F. Cotin, M. Niel, *et al.*, AIP Conf. Proc. **170**, 395 (1998).
3. J.-P. Dezalay, C. Barat, R. Talon, *et al.*, in *Gamma-Ray Bursts,* Ed. by W. S. Paciesas and C. J. Fishman (American Inst. of Physics, New York, 1992), vol. 304.
4. J.-P. Dezalay, J.-L. Atteia, C. Barat, *et al.*, Astron. Astrophys. **286**, 103 (1994).
5. J. C. Higdon and M. Schmidt, Astrophys. J. **355**, 13 (1990).
6. K. Hurley, in *Gamma-Ray Bursts,* Ed. by W. S. Paciesas and G. J. Fishman (American Inst. of Physics, New York, 1992), p. 3.
7. C. Kouveliotou, C. A. Meegan, G. J. Fishman, *et al.*, Astrophys. J. Lett. **413**, L101 (1993).
8. E. P. Mazets and S. V. Golenetskiĭ, Itogi Nauki Tekh., Ser. Astron. **32**, 16 (1987).
9. C. A. Meegan, G. N. Pendleton, M. S. Briggs, *et al.*, Astrophys. J., Suppl. Ser. **106**, 65 (1996).
10. I. Mitrofanov, A. Pozanenko, J.-L. Atteia, *et al.*, in *Bursts Observations, Analyses and Theories,* Ed. by C. Ho *et al.* (Cambridge Univ. Press, Cambridge, 1992), p. 203.
11. Y. Ogasaka, T. Murakami, J. Nishimura, *et al.*, Astrophys. J. Lett. **383**, L61 (1991).
12. W. S. Paciesas, C. A. Meegan, G. N. Pendleton, *et al.*, Astrophys. J., Suppl. Ser. **122**, 465 (1999).
13. V. Petrosian, Astrophys. J. **251**, 727 (1981).
14. B. Schaefer, B. Teegarden, S. Fantasia, *et al.*, Astrophys. J., Suppl. Ser. **92**, 285 (1994).
15. M. Schmidt, J. C. Hueter, and G. Hueter, Astrophys. J. Lett. **329**, L85 (1988).
16. O. V. Terekhov, D. V. Denisenko, V. A. Lobachev, *et al.*, Pis'ma Astron. Zh. **20**, 323 (1994) [Astron. Lett. **20**, 265 (1994)].
17. O. V. Terekhov, D. V. Denisenko, V. A. Lobachev, *et al.*, Pis'ma Astron. Zh. **21**, 83 (1995a) [Astron. Lett. **21**, 73 (1995a)].
18. O. Terekhov, R. Sunyaev, D. Denisenko, *et al.*, in *Proceedings of the IAU Colloquium No. 151 "Flares and Flashes,"* Ed. by J. Gremer, H. W. Duerbeck, and R. E. Gershberg (Springer-Verlag, Berlin, 1995); Lect. Notes Phys. **454**, 353 (1995b).
19. A. Yu. Tkachenko, O. V. Terekhov, R. A. Sunyaev, *et al.*, Pis'ma Astron. Zh. **24**, 833 (1998) [Astron. Lett. **24**, 722 (1998)].

Translated by G. Rudnitskiĭ